Cargo sorting to lysosome-related organelles regulates siRNA-mediated gene silencing

Dinari A. Harris, Kevin Kim, Kenji Nakahara, Constanza Vásquez-Doorman, and Richard W. Carthew

Department of Molecular Biosciences, Northwestern University, Evanston, IL 60208

Mammals lacking BLOC-3 have impaired formation of melanosomes, a type of lysosome-related organelle (LRO), and, in earlier work, we found that a subunit of the BLOC-3 complex inhibits loading of Argonaute (Ago) proteins with small ribonucleic acids (RNAs) in *Drosophila melanogaster* cells. Small RNAs such as small interfering RNAs (siRNAs) direct Ago proteins to repress the stability of messenger RNA transcripts. In this paper, we show that BLOC-3 is required for biogenesis of *Drosophila* LROs called pigment granules. Other complexes that sort cargo to pigment LROs also negatively regulate siRNA activity. However, regulation is not obligately linked to biogenesis of LROs but instead to specific cargo-sorting processes. Negative regulation is also not linked to sorting into all LROs but only a specific class of pigment LRO. Thus, regulation of siRNA activity is tied to sorting of specific types of cargo to particular LROs.

Introduction

Posttranscriptional gene silencing by small noncoding RNAs is a widespread mechanism to regulate gene expression in eukaryotes. siRNAs inhibit virus replication, transposon replication, and select protein-coding genes (Carthew and Sontheimer, 2009). Biogenesis of siRNAs requires the Dicer RNase III enzyme, which generates 21–23-nt siRNA duplexes from longer double-stranded RNA (dsRNA) precursors (Bernstein et al., 2001; Elbashir et al., 2001). Small RNA duplexes are then loaded from Dicer into an Argonaute (Ago) protein, where they unwind and only one RNA strand remains associated (Schwarz et al., 2003; Pham et al., 2004; Tomari et al., 2004; Kim et al., 2007). This ribonucleoprotein complex can potentially form base pair interactions between the guide siRNA strand and cytoplasmic mRNA transcripts. If base pairing is perfect across the center of the guide RNA, Ago cleaves the mRNA transcript (Schwarz et al., 2004). This is the primary mechanism by which siRNAs inhibit their target genes.

In one sense, Ago activity is highly dynamic in that different types of siRNAs can load or unload, generating complexes of considerable diversity and specificity. However, it is not as clear how Ago activity is regulated at the cellular level. Surprisingly, this can occur in a manner linked to membrane trafficking. Mammalian Dicer and Ago2 are found to be associated with intracellular membranes (Cikaluk et al., 1999; Lugli et al., 2005; Gibbings et al., 2009), and Ago2 was initially characterized as a Golgi- and ER-associated protein (Cikaluk et al., 1999). Further evidence has come from studies in *Drosophila melanogaster*. A genetic screen identified *Drosophila HPS4* (*dHPS4*) as an antagonist of siRNA-mediated silencing (Lee et al., 2009). Loss of *dHPS4* results in enhanced loading of siRNAs into Ago2 and increased Ago2 activity. Mammalian HPS4 protein is a subunit of the BLOC-3 complex, which mediates sorting of cargo proteins to lysosome-related organelles (LROs) such as melanosomes (Nguyen et al., 2002; Suzuki et al., 2002; Chiang et al., 2003; Martina et al., 2003; Nazarian et al., 2003). Genetic studies of mouse models for Hermansky-Pudlak syndrome (HPS), a human disorder associated with albinism, have implicated BLOC-3 as an important mediator of melanosome formation (Nguyen et al., 2002; Suzuki et al., 2002).

Functional LROs are generated by a multistep process in which an immature organelle forms and then matures by acquiring specialized cargo proteins. Proteins destined for residence in LROs flow from the trans-Golgi network and early endosomes to their final destination via transport vesicles that pinch

Correspondence to Richard W. Carthew: r-carthew@northwestern.edu

D.A. Harris's present address is National Institutes of Health, Bethesda, MD 20892.

K. Kim's present address is Harvard Medical School, Boston, MA 02115.

K. Nakahara's present address is Hokkaido University, Sapporo 060-0808, Japan.

Abbreviations used in this paper: dsRNA, double-stranded RNA; HPS, Hermansky-Pudlak syndrome; LRO, lysosome-related organelle; qPCR, quantitative PCR; UAS, upstream activating sequence.

The Rockefeller University Press $30.00
J. Cell Biol. Vol. 194 No. 1 77–87
www.jcb.org/cgi/doi/10.1083/jcb.201102021

off of donor organelles and fuse with acceptor organelles (Raposo et al., 2007). Vesicles carry a specific set of cargo proteins as part of the process. Delivery of cargo uses transport vesicles coated with the AP-3 adapter complex, which functions to sort cargo from early endosomes to LROs (Bonifacino and Glick, 2004; Raposo et al., 2007). Additional sorting complexes mediate sorting of LRO cargo. BLOC-1 and BLOC-2 sort cargo from early endosomes to melanosomes in a pathway that is distinct from the AP-3 pathway (Raposo and Marks, 2007). BLOC-3 appears to function independently of AP-3 and the other biogenesis of LRO complexes (BLOCs) in sorting protein to melanosomes. However, BLOC-3 function is not limited to LRO biogenesis; BLOC-3–deficient fibroblasts exhibit abnormal lysosome distribution, suggesting a role in lysosome motility (Falcón-Pérez et al., 2005). Rab GTPases are well-known regulators of vesicular transport, and Rab32 and Rab38 have been directly implicated in trafficking to LROs (Raposo and Marks, 2007). They are highly homologous proteins that are expressed in a limited set of cell types, including melanocytes (Di Pietro and Dell'Angelica, 2005; Huizing et al., 2008). Ubiquitous Rab proteins also appear to regulate LRO biogenesis (Hirosaki et al., 2002; Jordens et al., 2006). GTP-bound Rabs can associate with the homotypic fusion and vacuole protein sorting (HOPS) protein complex, which promotes lysosome membrane fusion events by interacting with the SNARE machinery (Raposo and Marks, 2007). The HOPS complex is also required for melanosome biogenesis, though its mechanism is not well understood.

We previously found that dHPS4 inhibits siRNA loading of Ago2 and its consequent efficacy for gene silencing (Lee et al., 2009). Cytoplasmic distribution of the Ago protein was also dependent on dHPS4, prompting us to hypothesize that its effects on Ago distribution and activity were possibly caused by lysosome motility. However, it was also possible that its effects were a result of a connection with cargo trafficking to *Drosophila* LROs. *Drosophila* orthologues for BLOC-1, BLOC-2, AP-3, Rab38, and HOPS proteins are required for biogenesis of a class of LROs called pigment granules (Sevrioukov et al., 1999; Krämer, 2002; Ma et al., 2004; Falcón-Pérez et al., 2007; Syrzycka et al., 2007; Cheli et al., 2010). These observations suggest an evolutionarily conserved role for these complexes in the biogenesis of LROs. Here, we test the model that cargo sorting to LROs is the primary mechanism by which Ago2 is negatively regulated. Specifically, we wanted to know whether *Drosophila* BLOC-3 is involved in biogenesis of LROs, whether other sorting complexes regulate the siRNA silencing pathway, and, if so, how sorting is coupled to Ago2 activity.

Results

Role of dHPS4 in pigment LRO biogenesis

Eye pigment cells of *Drosophila* contain specialized LROs called pigment granules, which can be classified into two distinct types based on pigment composition and cell type (Nolte, 1961; Lloyd et al., 1998). Type I granules contain ommochrome pigment and are found in primary, secondary, and tertiary pigment cells. Type II granules contain drosopterin pigment and are only found in secondary and tertiary pigment cells. Mutations that disrupt biogenesis of one granule type have no effect on the other type, suggesting that their formation is independent of one another (Nolte, 1961; Shoup, 1966). Consistent with this idea, biogenesis of ommochrome LROs precedes drosopterin LROs by many hours during cell differentiation (Shoup, 1966). Genetic loss of either BLOC-1, BLOC-2, AP-3, Rab38, or the HOPS complexes results in aberrant formation of both types, indicating common pathways of cargo sorting to both LROs (Sevrioukov et al., 1999; Krämer, 2002; Ma et al., 2004; Falcón-Pérez et al., 2007; Syrzycka et al., 2007; Cheli et al., 2010). However, each LRO type is differentially dependent on certain types of complexes.

It was of interest to determine whether the *Drosophila* BLOC-3 complex is also required for pigment LRO biogenesis. We measured ommochrome pigment level in a *dHPS4* mutant, and the mutant showed a significant decrease in ommochrome compared with that of wild type (Fig. 1 A). Drosopterin pigment levels were modestly reduced (15%) in the mutant (Fig. 1 B). Other *dHPS4* alleles showed similar effects (unpublished data). The mouse BLOC-3 complex functions in an independent pathway from the AP-3 and BLOC-2 pathways. We wished to determine whether BLOC-3 also has an autonomous relationship with other sorting complexes in *Drosophila* pigment cells. Therefore, we generated double mutants of *dHPS4* and other *HPS* genes and assayed levels of ommochrome pigment in the double mutants (Fig. 1 A). The *garnet* (*g*) and *ruby* (*rb*) genes encode two subunits of the AP-3 complex (Krämer, 2002). Ommochrome levels in *g dHPS4* and *rb dHPS4* double mutant flies were lower than those in the single mutants alone, indicating that AP-3 and BLOC-3 independently regulate ommochrome LRO biogenesis. The *pink* (*p*) gene encodes for a subunit of BLOC-2. The *p dHPS4* double mutants also showed less ommochrome than that of the single mutants alone. Similar additive interactions were observed between *dHPS4* and *claret* (*ca*), encoding a guanine nucleotide exchange factor for Rab GTPases, and between *dHPS4* and *carnation* (*car*), encoding a core subunit of the HOPS complex (Fig. 1 A). Interestingly, loss of *dHPS4* had no effect on ommochrome levels when the Rab38 gene *lightoid* (*ltd*) was mutated. This result indicates that *ltd* is epistatic to *dHPS4*, and, therefore, Rab38 and BLOC-3 function in a common pathway with Rab38 downstream of BLOC-3.

We also examined drosopterin pigment levels in the double mutants (Fig. 1 B). Additive interactions were detected between *dHPS4* and *g*, *rb*, *ca*, and *ltd*. In contrast, when either the *car* subunit of HOPS or the *p* subunit of BLOC-2 was mutant, loss of *dHPS4* had no effect on drosopterin levels. This suggests that HOPS, BLOC-2, and BLOC-3 act in a common sorting pathway for drosopterin LROs. Collectively, these results show a complex hierarchy of interactions between dHPS4 and other HPS proteins, consistent with BLOC-3 functioning in biogenesis of both classes of pigment LROs.

AP-3 and BLOC-2 negatively regulate the siRNA pathway

Because dHPS4 participates in pigment LRO biogenesis, we wished to know whether its effects on siRNA activity were

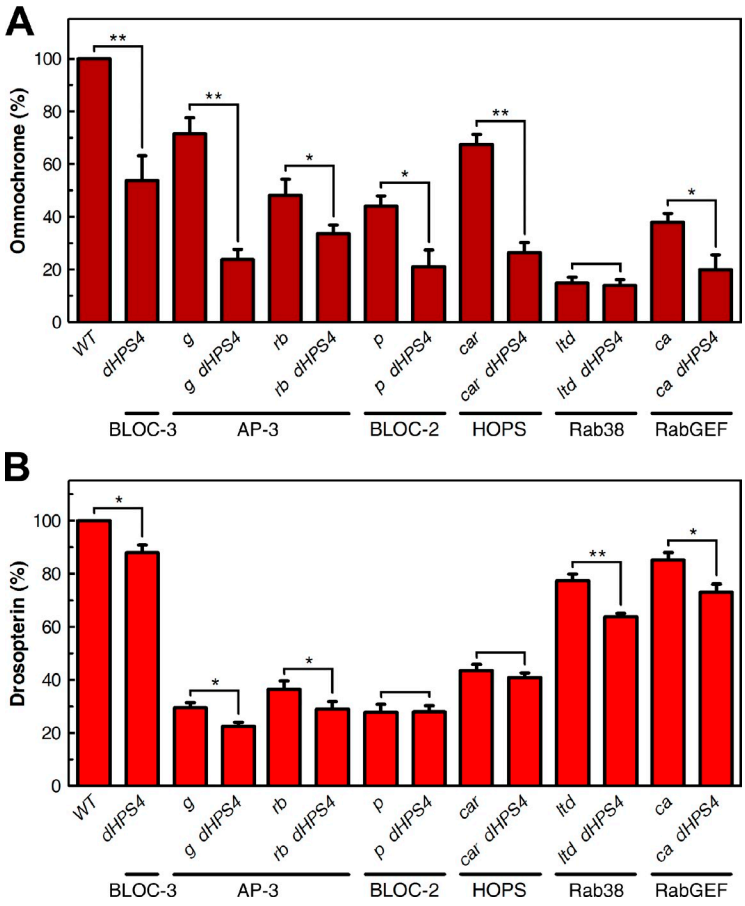

Figure 1. **Function of dHPS4 in pigment biogenesis.** (A) Ommochrome pigments from wild-type (WT), *dHPS4*^{W515X}, *g*^{1}, *rb*^{1}, *p*^{1}, *car*^{1}, *ca*^{1}, and *ltd*^{1} flies. Values are expressed as percentages of the pigment content of wild-type flies and represent means of three to five independent determinations. (B) Drosopterin pigments from wild-type and mutant flies. Values are expressed as percentages of the pigment content of wild-type flies and represent means of three to five independent determinations. (A and B) Error bars represent SDs. In all statistical tests, significance was determined by a Student's *t* test: *, $P < 0.05$; **, $P < 0.01$.

linked to its LRO function. To test this hypothesis, we examined the effects of other sorting complexes on siRNA activity, reasoning that if silencing is linked to LRO biogenesis, these other complexes would also inhibit silencing. To assay siRNA activity, we expressed a transgene (*GMR-wIR*) that silences expression of the endogenous *white* gene in the eye. It does so by driving eye-specific synthesis of a hairpin dsRNA corresponding to a segment of *white* mRNA (Lee and Carthew, 2003). Gene silencing was assayed by determining *white* mRNA levels in heads. In a wild-type background, *GMR-wIR* induced a twofold reduction in *white* mRNA (Fig. 2 A). The effect was not greater because *white* mRNA expressed in the brain was not repressed by the eye-specific siRNAs. Loss of *g*, *rb*, *p*, or *ca* resulted in enhanced repression of *white* mRNA in a manner completely dependent on the expression of *white* siRNAs (Fig. 2 A). To confirm these results, we measured *white* activity in the eye by assaying drosopterin pigment levels; *white* is a pigmentation gene required for drosopterin synthesis. *GMR-wIR* induced a 90-fold reduction in *white* gene activity (Fig. 2 B). In the absence of *GMR-wIR*, the *dHPS4*, *g*, *p*, and *ca* mutants had modest effects on drosopterin as noted earlier (Fig. 1). However, in the presence of *GMR-wIR*, the repression of *white* activity was enhanced manyfold by *dHPS4*, *g*, *p*, and *ca* (Fig. 2 B).

We tested whether these effects on siRNA activity extended to other target genes. Eye-specific expression of a hairpin RNA against the *argos* gene resulted in a weak mispatterning of the eye surface as a result of cell apoptosis (Fig. 2 C). This mispatterning was modestly enhanced when *rb* or *p* was mutant and was much more enhanced in a *ca* mutant background (Fig. 2, D–G). None of the mutants had any effect on eye patterning in the absence of *argos* siRNAs (unpublished data). We also expressed a hairpin RNA against the *brown* (*bw*) gene, resulting in a fivefold reduction in *bw* mRNA levels (Fig. 2 H). This reduction was enhanced in a *g*, *p*, or *ca* mutant background. Loss of *rb* had no effect on *bw* silencing. Similar effects were seen with RNAi knockdown of the *purple* (*pr*) gene (Fig. 2 H). The stronger dependence of *white* and *argos* RNAi on *rb* is countered with stronger dependence of *bw* and *pr* RNAi on *g*. These data suggest that AP-3 subunits might contribute differentially to gene targeting in some unknown way.

We also tested the effect of the HOPS complex on siRNA activity. We did so by assaying silencing activity in a *car* mutant, which inactivates the core VPS22A subunit of HOPS. Interestingly, the *car* mutant did not enhance silencing of *white* by *GMR-wIR* (Fig. 2, A and B). This result indicates that pigment LROs themselves are not the key determinants of siRNA regulation, as the *car* mutant allele significantly impairs biogenesis of both types of pigment LROs (Fig. 1; Sevrioukov et al., 1999). Regulation appears to be tied to specific cargo-sorting processes that depend on BLOC-2, BLOC-3, and AP-3 but not the HOPS complex.

Ommochrome LROs specifically inhibit siRNA activity

There are two types of pigment LROs, and it is possible that cargo sorting to one type or both types regulates siRNA activity.

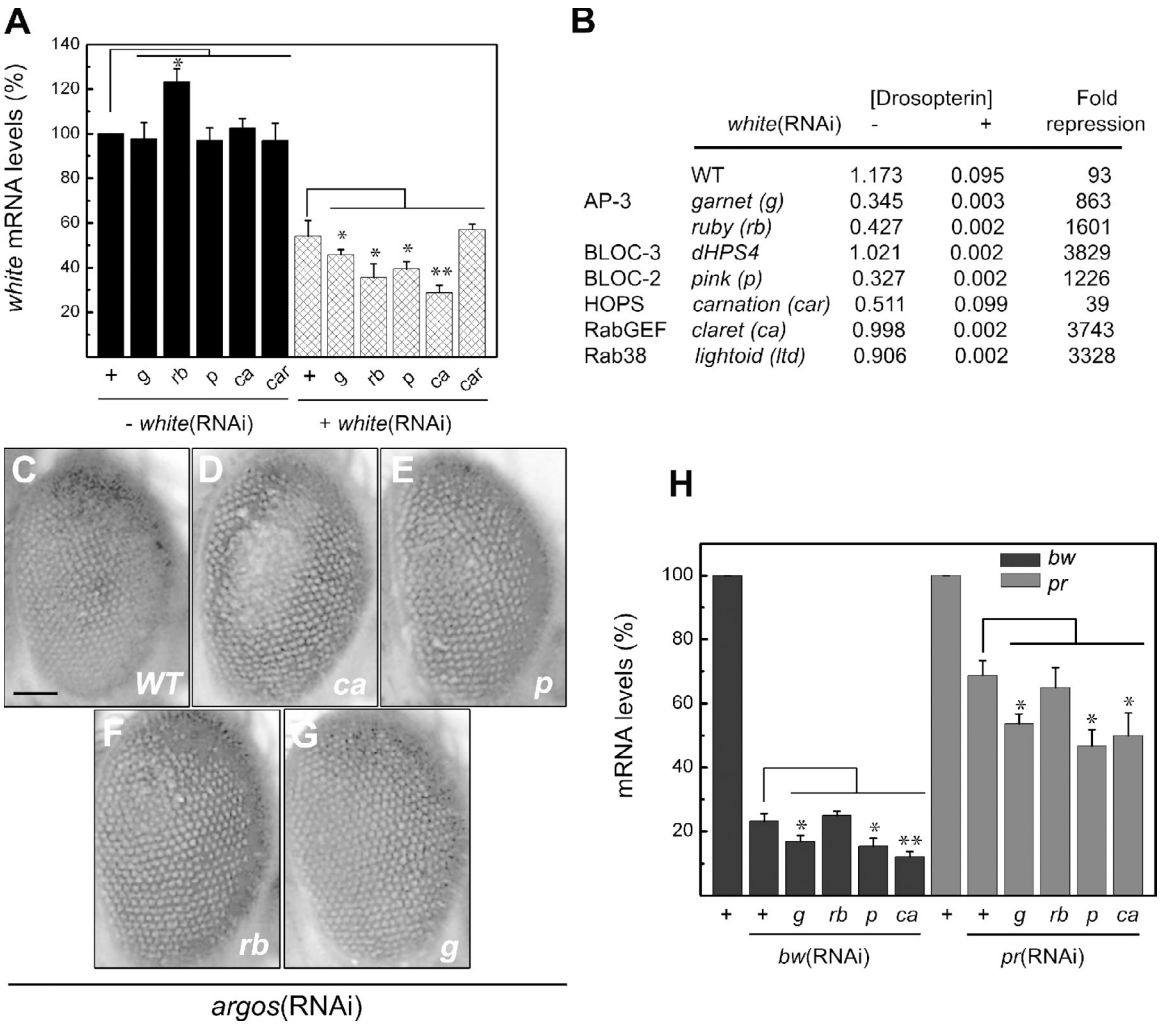

Figure 2. **Pigment LRO-sorting genes regulate RNA silencing in vivo.** (A) The level of *white* mRNA in the presence or absence of *GMR-wIR* to induce *white*(RNAi). Levels are shown from flies in the following different genetic backgrounds: +, g^1, p^1, rb^1, car^1, and ca^1. RNA values were measured by real-time qPCR and normalized to Rpl32 mRNA. Statistical significance was determined by a Student's *t* test: *, P < 0.05; **, P < 0.01. (B) Repression of *white* activity as measured by drosopterin concentration. Drosopterin levels (A_{495} absorbance) are shown in different genetic backgrounds, as indicated. (right column) Fold repression of drosopterin by *white*(RNAi) expressed as a normalized ratio. This ratio normalizes for the differences in starting material and extract volumes between *white*(RNAi) samples and non-RNAi samples that were used in the experiment. (C–G) Compound eyes of flies with *GMR>argsIR*, which causes mildly mispatterned facets in a wild-type (WT) background (C) and a blistering of facets in the medial-posterior region in *ca* (D), *p* (E), *rb* (F), or *g* (G) mutants. (H) Real-time qPCR measurements of the relative levels of *bw* mRNA with and without *GMR>bwIR* and *pr* mRNA with and without *GMR>prIR*. Levels in different mutant backgrounds are as indicated. Statistical significance was determined by a Student's *t* test: *, P < 0.05; **, P < 0.01. Errors bars represent SDs. Each sample was performed in quadruplicate. Bar, 100 µm.

To test this hypothesis, we examined various mutants that specifically impair biogenesis of the ommochrome or drosopterin LROs. Biogenesis of these LROs is not only dependent on cargo-sorting complexes but also the cargo proteins themselves (Nolte, 1961; Shoup, 1966). If ommochrome cargo genes are mutant, biogenesis of ommochrome LROs is specifically blocked. A specific effect on drosopterin LROs is also seen with drosopterin cargo mutations. We examined different genes in each class to determine whether ommochrome or drosopterin LRO cargo affects the siRNA pathway. We measured the effect of such mutants on *white*(RNAi) by measuring pigment levels in a *GMR-wIR* background. Loss of ommochrome genes *cardinal* (*cd*), *karmoisin* (*kar*), *scarlet* (*st*), *cinnabar* (*cn*), or *vermillion* (*v*) strongly enhanced the repressive effect of *GMR-wIR* on *white* activity (Fig. S1). Surprisingly, loss of drosopterin genes *bw* or *pr* did not enhance the repressive effect of *GMR-wIR* but in fact strongly suppressed *white*(RNAi) (Fig. S1). These results suggest that siRNA activity is specifically inhibited by the ommochrome pathway, whereas the drosopterin pathway potentiates siRNA activity.

To further explore the relationship between the ommochrome LRO pathway and the siRNA pathway, we focused on one cargo protein that acts inside ommochrome LROs. The product of the *cd* gene converts 3-hydroxykynurenine (3-HOK) into ommochrome pigment (Howells et al., 1977; Mackenzie et al., 2000). We isolated new mutant alleles of *cd* (Fig. 3 A). Using these new alleles, we positionally localized the gene to CG6969, which encodes a heme peroxidase (Fig. 3 B). We sequenced CG6969 in five independent mutants, and each mutant had base changes that significantly altered the predicted protein product (Fig. 3 B).

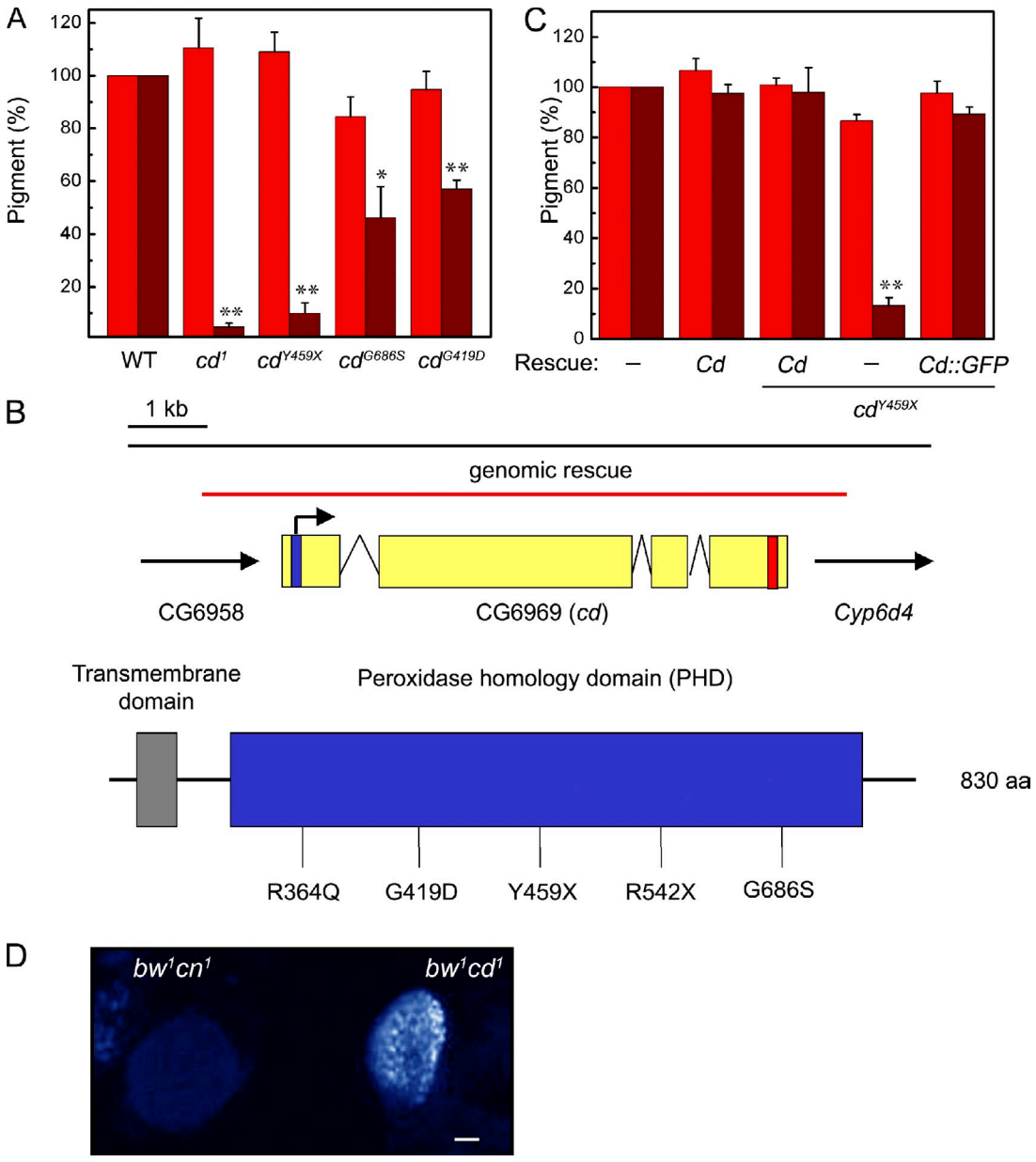

Figure 3. ***cd* mutants affect ommochrome biosynthesis in *Drosophila*.** (A) Levels of drosopterin (red bars) and ommochrome (brown bars) in wild-type (WT) and four independent *cd* mutant alleles. (B) The *cd* gene and protein. (top) The *cd* CG6969 transcription unit. Exons are presented as yellow boxes, and the direction of transcription is indicated. The position of start and stop codons are indicated by vertical blue and red lines, respectively. The range of the *cd* genomic rescue region is shown as a red line. (bottom) The predicted Cd protein product showing the transmembrane domain in gray and the heme peroxidase domain in blue. The positions of five new *cd* mutations are indicated, two generating nonsense stop codons (X) and three generating missense mutations. (C) Rescue of the eye pigment defect in cd^{Y459X} mutant flies carrying *GMR-Gal4/UAS-Cd* or *GMR-Gal4/UAS-Cd::GFP* transgenes, indicated as Cd and Cd::GFP, respectively. (A and C) Errors bars represent SDs. Each sample was performed in triplicate. Statistical significance was determined by a Student's *t* test: *, $P < 0.05$; **, $P < 0.01$. (D) Accumulation of the autofluorescent 3-HOK in the adult eye is specifically detected in the bw^1cd^1 double mutant. A control bw^1cn^1 double mutant shows no autofluorescence. Bar, 200 µm.

Two alleles contained premature stop codons that would produce truncated proteins, lacking an intact peroxidase domain. The two mutations likely represent null alleles. To confirm that CG6969 corresponded to *cd*, we expressed the CG6969 cDNA in eye cells. This completely rescued the phenotype associated with a homozygous *cd*-null mutant (Fig. 3 C). A genomic fragment that spans the CG6969 transcription unit (Fig. 3 B) also rescued the *cd*-null phenotype (not depicted). To confirm that Cd converts 3-HOK to ommochrome, we looked for the accumulation of 3-HOK in the adult eye of *cd* mutants by taking advantage of the unique blue autofluorescent properties of 3-HOK (Siddiqui and Babu, 1980). We observed strong blue autofluorescence in the eyes of *cd* mutants (Fig. 3 D).

The Cd protein is predicted to have two functional domains (Figs. 3 B and S2). There is a transmembrane domain located 45 amino acids from the amino terminus, suggesting that the product might be an integral membrane protein. At the carboxy terminus is the heme peroxidase domain. If the amino-terminal domain targets the protein to membranes, we predicted the protein would be membrane localized. Therefore,

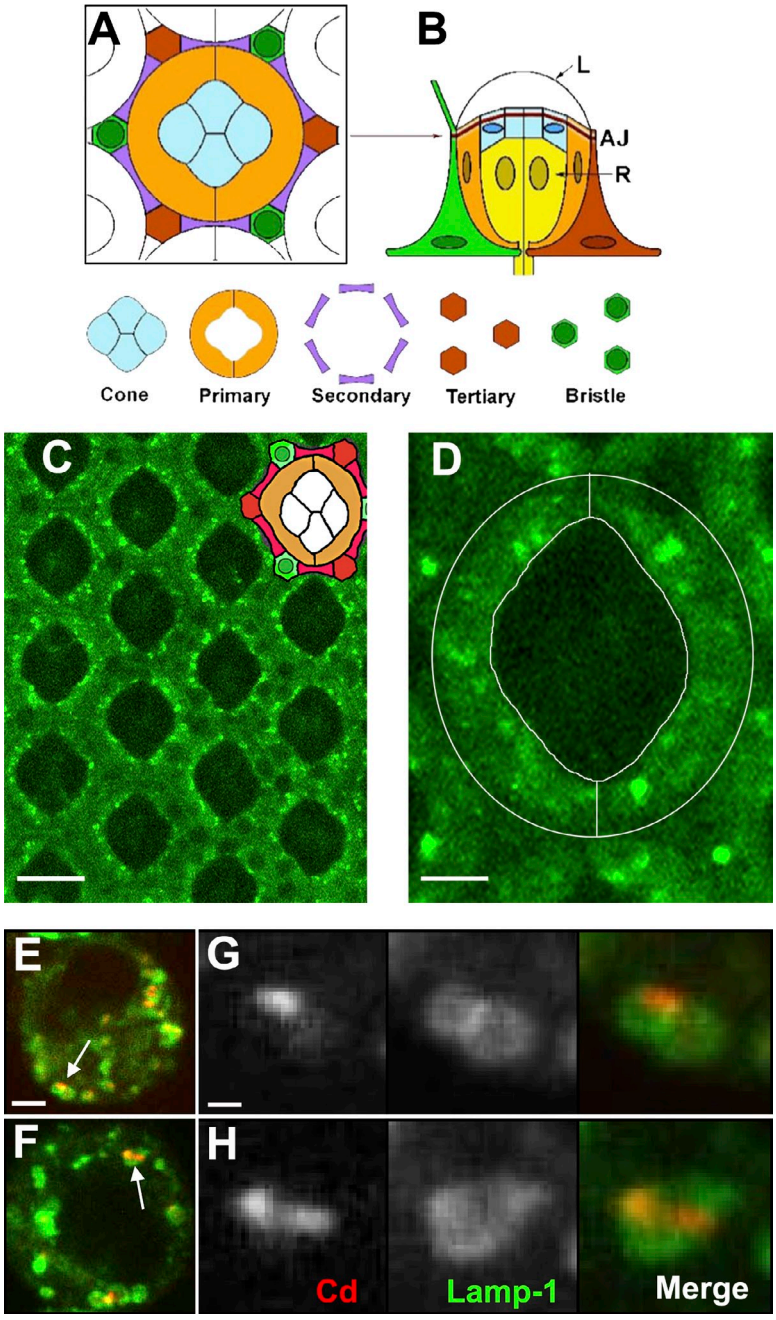

Figure 4. **Cd protein localization.** (A) A cross section schematic of one *Drosophila* pupal ommatidium, with the core of cone and primary pigment cells and the frame of secondary and tertiary/bristle cells. (B) A side view of an ommatidium with photoreceptor cells (R) below the adherens junction (AJ) and the lens (L) above it. (C) Localization of Cd::GFP (green) in a cross section through several ommatidia. (top right) A camera lucida outline of a single ommatidium. Although the *GMR>Cd::GFP* gene is expressed in all cells, Cd::GFP is not uniformly abundant in all cells. It is particularly abundant in primary pigment cells. (D) Subcellular localization of Cd::GFP (green) in a cross section through one ommatidium. The primary pigment cells are individually shaped like half rings, as marked by white lines. (E and F) Subcellular localization of Cd::RFP (red) and Lamp-1::GFP (green) in two representative S2 cells. The cell nuclei are unstained with both markers. (G and H) Subcellular vesicles that are magnified from images in E and F, respectively, and highlighted with arrows. Each fluorescence signal is shown separately and merged. Bars: (C) 10 µm; (D) 3 µm; (E and F) 2 µm; (G and H) 0.4 µm.

we examined the subcellular distribution of the protein by fusing it to a fluorescent protein (either GFP or RFP) at the carboxy terminus. The GFP fusion protein was fully functional as shown by transgene rescue of the *cd* mutant phenotype in the *Drosophila* eye (Fig. 3 C). The GFP fusion protein was then visualized by confocal microscopy of eye tissue. Each facet or ommatidium of the eye contains 20 cells in a stereotyped pattern (Fig. 4, A and B). Even though the fusion gene was transcribed in all eye cells, the primary pigment cells had robust levels of protein that was localized to the cytoplasm (Fig. 4 C). Neighboring cone cells were bereft of the protein, suggesting some posttranscriptional control of protein abundance. In the pigment cells, Cd::GFP protein was concentrated in vesicles (Fig. 4 D). To identify which vesicles contained the protein, we coexpressed Cd::RFP in S2 cells with various markers for cytoplasmic organelles. Cd::RFP protein localization specifically overlapped with organelles marked by Lamp-1::GFP (Fig. 4, E–H). Lamp-1 is a type I integral membrane protein found in the limiting membrane of late endosomes and lysosomes (Lloyd et al., 1998). Cd::RFP protein was not uniformly distributed on lysosomal membranes but rather was localized to subdomains overlapping and interior to Lamp-1::GFP, suggesting that the Cd::RFP carboxy terminus is lumenal. This interpretation is consistent with structural features of Cd that suggest it is a type II membrane protein: there is no amino-terminal signal sequence, there is a proximal transmembrane domain, and there is a strong charge differential between the flanking sequences directed positive to negative

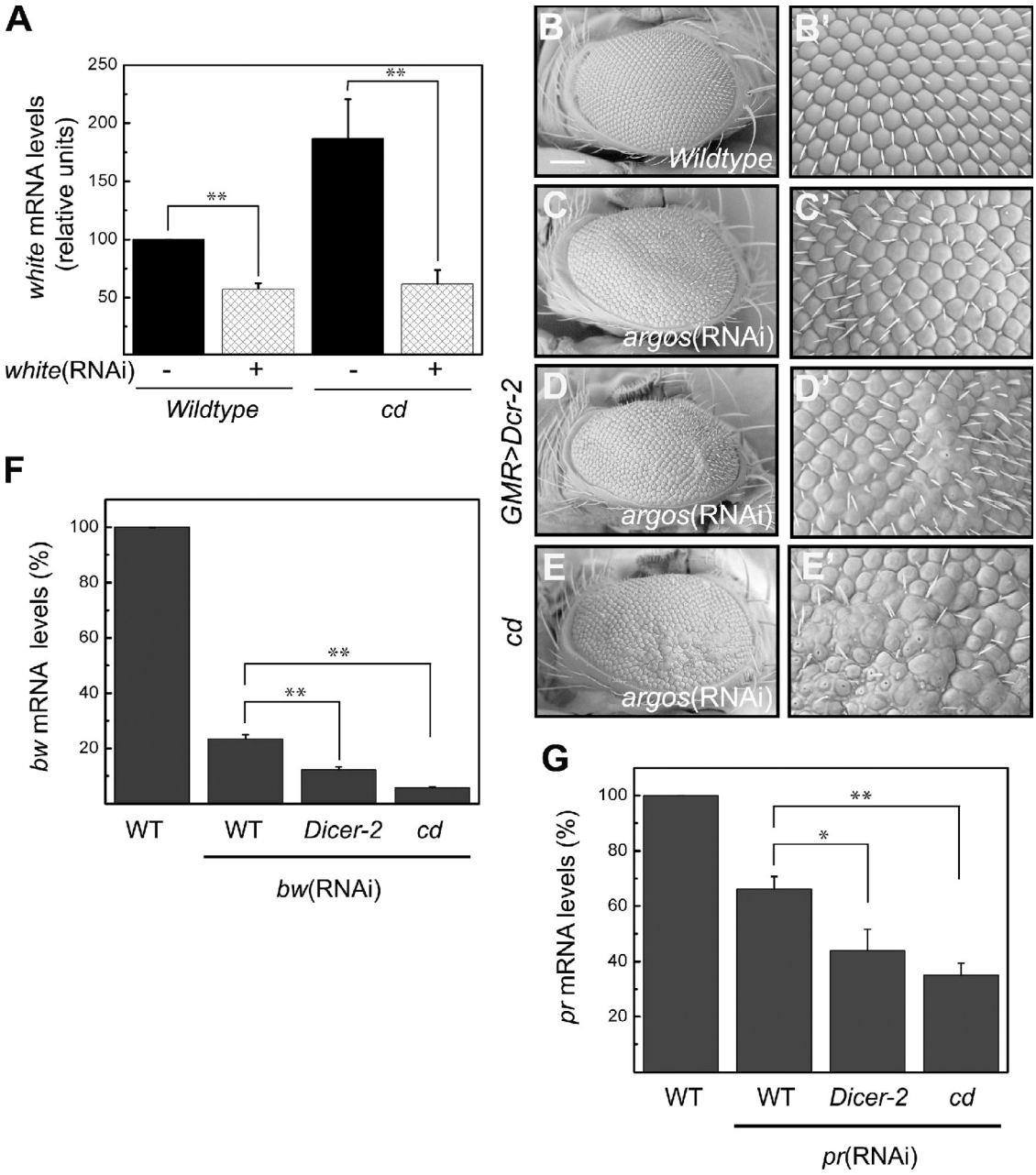

Figure 5. **Cd is an inhibitor of siRNA-mediated silencing.** (A) The level of *white* mRNA in the presence or absence of *GMR-wIR* to induce *white*(RNAi). Levels are shown from flies in a wild-type and cd^{Y495X} background. RNA values were measured by real-time qPCR and normalized to Rpl32 mRNA. Statistical significance was determined by a Student's *t* test: **, P < 0.01. (B–E) Scanning electron microscopy of eyes from wild-type (B) and *GMR>argosIR* (C–E) flies shown under low magnification in the left column and higher magnification in the right column. Mispatterning is worsened in a *GMR>Dicer-2* (D) and cd^{Y495X} mutant (E) background. (F) Silencing of *bw* head mRNA by eye-specific *bw* siRNAs made by *GMR>bwIR*. *GMR>Dicer-2* and *cd* mutant backgrounds are indicated. WT, wild type. (G) Silencing of *pr* head mRNA by eye-specific *pr* siRNAs made by *GMR>prIR*. *GMR>Dicer-2* and *cd* mutant backgrounds are indicated. Errors bars represent SDs. Each sample was performed in quadruplicate. For F and G, statistical significance was determined by a Student's *t* test: *, P < 0.05; **, P < 0.01. Bar: (B–E) 100 µm; (B'–E') 10 µm.

(Fig. S2; Hartmann et al., 1989). In summary, Cd protein is lysosome targeted in S2 cells, and its distribution in pigment cells suggests an LRO-restricted pattern.

Cd inhibits the siRNA pathway

We explored the connection between ommochrome cargo and siRNA activity by analysis of Cd. Loss of *cd* resulted in stronger repression of *white* head mRNA when *white* siRNAs were expressed in the eye (Fig. 5 A). This effect of *cd* on *white* gene silencing was also seen by monitoring *white* activity (Fig. S1). To confirm that the *cd* effect on silencing was mediated by siRNAs, we combined *cd* with a *dicer-2*–null mutation. Loss of *dicer-2* blocks the production of siRNAs in *Drosophila* (Lee et al., 2004). The enhanced silencing of *white* by *cd* was completely negated by *dicer-2*; flies had an eye color resembling simple loss of *cd* (Fig. S3).

We determined whether enhanced gene silencing by *cd* mutants also applied to other target genes. Silencing of *argos* in eye

tissue results in apoptosis of cells and a weakly mispatterned eye (Fig. 5, B and C). As has been previously reported, *argos*(RNAi) can be enhanced by overexpression of *Dicer-2*, resulting in greater mispatterning of the eye (Fig. 5 D; Dietzl et al., 2007). When *argos*(RNAi) was induced in a *cd* mutant background, eye mispatterning was also enhanced (Fig. 5 E). This interaction was not the result of a functional relationship between *cd* and *argos* to control apoptosis. We generated *cd argos* double mutants and found eye patterning was not further impaired compared with the single mutants (Fig. S4). Thus, *cd* mutants enhance the silencing potency by siRNAs against *argos*. We also examined siRNA silencing of the *bw* and *pr* genes in the eye. In the presence of eye-specific hairpin RNAs, *bw* and *pr* mRNA levels were reduced 80 and 40%, respectively (Fig. 5, F and G). Knockdown of both mRNAs was significantly enhanced by either overexpressing *Dicer-2* or loss of *cd*. There was no reduction of *bw* or *pr* mRNA in a *cd* mutant when the RNA hairpins were not expressed in the eye (unpublished data). Collectively, these data indicate that *cd* mutants enhance the siRNA-mediated silencing pathway.

Ago2 loading is specifically inhibited by Cd

Although Cd is an ommochrome cargo protein in pigment cells, the *cd* gene is expressed in many more tissues than the eye (Fig. S5). We observed *cd* mRNA expression in embryos, adult gonads, and malphigian tubules. Because the *cd* gene is expressed in embryos, we could use siRNA biochemistry to determine what steps in the silencing pathway are regulated by Cd. *Drosophila* embryos are an excellent model for eliciting silencing in vitro (Tuschl et al., 1999; Haley et al., 2003; Pham et al., 2004), and silencing can be broken into discrete biochemical steps, including dsRNA processing into siRNAs, siRNA loading into Ago2, and cleavage of target mRNA by Ago2/siRNA (Carthew and Sontheimer, 2009). We tested whether Cd affects dsRNA processing by incubating labeled dsRNA in cytoplasmic lysates made from *cd* mutant embryos and by monitoring siRNA production (Fig. 6 A). There was little difference in the rate of siRNA production between wild-type and *cd* mutant lysates, indicating that Cd does not significantly affect processing.

To examine Ago2 loading in *cd* mutant lysate, we used native gel electrophoresis to visualize loading complexes. Loading begins by recruitment of siRNA into the R2D2–Dicer2 initiator complex, which is composed of Dicer-2 and R2D2 proteins. This complex is converted into an intermediate RNA-induced silencing complex–loading complex, which then loads the siRNA into Ago2 (Carthew and Sontheimer, 2009). To address the effect of the *cd* mutant on Ago2 loading, we examined the abundance of these various complexes when associated with a labeled siRNA (Fig. 6 B). R2D2–Dicer2 initiator and RNA-induced silencing complex–loading complexes were detected at levels comparable with wild type, whereas loaded Ago2 was greatly elevated in *cd* mutant lysate. This result indicates that the mutant enables greater loading of Ago2 at the final step in the loading pathway. One possible explanation for greater loading in the *cd* mutant is that Ago2 is simply more abundant. To address this possibility, we assayed the level of Ago2 by Western blotting. Protein was unaffected in the *cd* mutant, suggesting that loading was enhanced through a different mechanism (unpublished data).

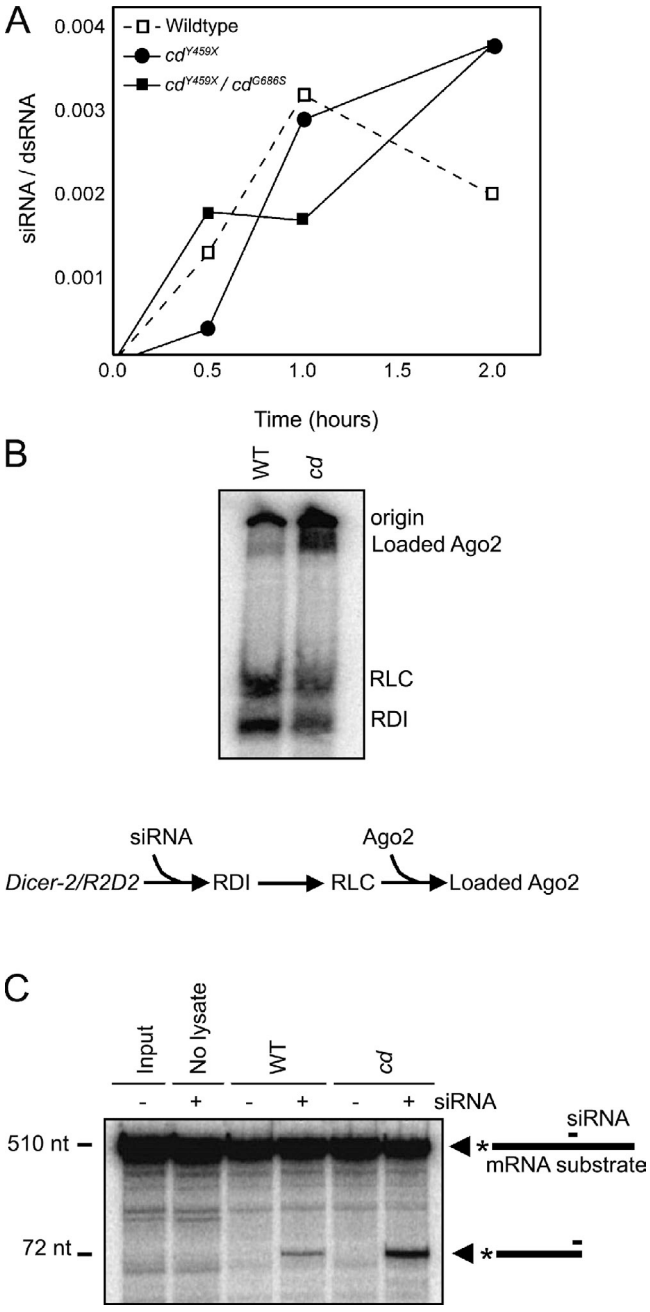

Figure 6. **Cd inhibits Ago2 loading.** (A) Processing of dsRNA substrate into siRNAs by cytoplasmic lysates from wild-type and *cd* mutant embryos. Normalized siRNA levels over time are plotted. (B) Ago2 loading in wild-type (WT) and *cd* mutant lysates. Radiolabeled siRNA was incubated with lysate, and labeled complexes were detected by native gel electrophoresis. Some label remains adhered to the origin of electrophoresis. The pathway of Ago2 loading is schematized below. RDI, R2D2–Dicer2 initiator; RLC, RNA-induced silencing complex–loading complex. (C) siRNA-induced mRNA cleavage in wild-type and *cd* mutant lysates. The 5′ labeled mRNA is cleaved upon incubation with lysate and siRNA, accumulating a 5′ cleavage product, as indicated after electrophoresis. Molecular weights of RNAs are indicated in nucleotides. The asterisks refer to the schematic of the molecular structure showing where the radioactive label is located.

If more Ago2 is loaded in a *cd* mutant, more Ago2 should be available to cleave target mRNA. We loaded an unlabeled siRNA into Ago2 by addition of the siRNA to lysate and then assayed Ago2 cleavage activity by incubation with an end-labeled mRNA

containing a complementary binding site. Cleavage was detected by the appearance of the end-labeled RNA fragment. The *cd* mutant lysate generated significantly more cleavage product than wild-type lysate (Fig. 6 C). The increase in cleavage activity (threefold) was comparable with the increase in loaded Ago2 (three- to fivefold), suggesting that *cd* enhances the loading of Ago2 but not its cleavage activity once loaded.

Discussion

The aim of this study is to determine how gene silencing is connected to membrane trafficking. We had observed that loss of dHPS4 protein enhanced siRNA loading into Ago2 and altered the distribution of Ago protein in cells (Lee et al., 2009). Knockdown of human HPS4 in HeLa cells had similar effects. HPS4 is required for LRO biogenesis and also for lysosome motility in cells lacking LROs (Wei, 2006). This raised the question of whether LRO trafficking or some other feature of organelle biology was responsible for siRNA regulation. To explore this question, we have determined that loss of *dHPS4* impairs production of eye pigments and affects pigmentation independent of the AP-3 and BLOC-2 cargo-sorting pathways. This observation is consistent with data from a mouse genetic study that found BLOC-3 to independently control melanosome biogenesis (Feng et al., 2002). Intriguingly, *dHPS4* acts genetically upstream of *ltd*, the *Drosophila* orthologue of Rab38, for ommochrome LRO production. Therefore, the conserved function of HPS4 for LRO biogenesis makes it plausible that LRO trafficking regulates siRNA activity.

This hypothesis was further tested by measuring siRNA activity when other LRO cargo-sorting complexes are disrupted. We found that disruption of the BLOC-2, AP-3, or Rab38 complexes leads to stronger gene silencing. However, disruption of the HOPS complex has no effect on silencing, which argues that the simple presence of the LRO compartment is not the regulatory determinant, as there are fewer pigment LROs when HOPS activity is compromised (Sevrioukov et al., 1999). The precise role of HOPS in LRO formation is not well understood, but other studies indicate that it tethers trafficking vesicles and organelles to late endosomes and lysosomes for fusion (Bonifacino and Glick, 2004; Raposo et al., 2007). If it performs analogous functions in LRO biogenesis, it would act downstream of AP-3 and BLOC-2, which are thought to function in linking transmembrane cargo (through cytoplasmic sorting signals) to vesicle formation on post-Golgi membranes. In melanocytes, AP-3 and BLOC-2 probably function in sorting cargo into vesicles from early endosomes. These results would indicate that the early steps of cargo sorting to the LRO compartment regulate siRNA activity. Ago proteins can physically associate with the exterior of Golgi and endosomes even though they are not transmembrane proteins (Cikaluk et al., 1999; Gibbings et al., 2009; Lee et al., 2009). One possibility is that Ago protein shuttles between organelles using preexisting sorting pathways, and its competence to load small RNAs is modulated by which compartment it is associated with. In this model, Ago2 associated with early endosomes is capable of loading siRNAs, but it is incapable of loading when shuttled away from early endosomes. Loss of AP-3 and other sorting complexes would block the shuttling process, whereas loss of HOPS would presumably not prevent shuttling away from endosomes. Another possibility is that Ago protein distributes between a free cytosolic pool that is capable of loading small RNAs and a membrane-bound pool that is not. The size of this membrane-bound pool might then be regulated by the magnitude and mode of cargo sorting.

Pigment cells contain two different pigment LROs: ommochrome and drosopterin pigment granules. Remarkably, sorting into ommochrome LROs inhibits loading of Ago2 with siRNAs, whereas drosopterin LRO sorting has the opposite effect. How do the two LROs differentially regulate silencing? One possibility is that negative regulation only occurs in cells that exclusively contain ommochrome LROs. However, siRNA silencing of drosopterin gene expression is enhanced by mutants that disrupt ommochrome LROs. Thus, negative regulation is occurring in cells that contain both types of LROs. Another possibility is that cargo exclusive to the ommochrome LRO regulates Ago2 in a negative manner. Greater Ago2 loading is observed when the ommochrome cargo protein Cd is not produced, lending support to this possibility. The Cd protein appears to be anchored to the ommochrome-limiting membrane, with a cytoplasmic tail of 45 amino acids.

In conclusion, siRNA activity is regulated by cargo sorting to LROs. Regulation occurs by controlling the level of Ago2 loaded with siRNAs and, thereby, the level of active Ago2. Regulation is linked to specific steps in cargo sorting and specific types of cargo. Thus, it is not likely a general property of all cell types but might be particularly significant in certain cell types such as pigment cells and possibly neurons. The reason why this regulation exists is tantalizingly mysterious, but the fact that it is conserved between *Drosophila* and humans argues that the reason is of general importance.

Materials and methods

Genetics

Mutants in the pigment synthesis pathway and transport pathways were obtained from the Bloomington Stock Center. The alleles used were g^1, rb^1, p^1, ltd^1, ca^1, car^1, cd^1, bw^1, cn^1, st^1, kar^{20}, v^1, pr^1, and $argos^{rlt}$. New *cd* alleles were isolated from a screen for RNAi enhancer mutations (Lee et al., 2004). Allele designations are according to their amino acid change. The $dicer\text{-}2^{L811fsX}$ and $dHPS4^{W515X}$ are null alleles as described in Lee et al. (2004, 2009). A genomic transgene encompassing CG6969 (*cd*) was made by subcloning a 3.5-kb fragment into P[acman] (Venken et al., 2006). To generate an upstream activating sequence (UAS) transgene, the coding sequence from a *cd* cDNA was cloned via Gateway (Carnegie Institution of Washington) into the pPW UAS transgene vector. We obtained the cDNA from the Drosophila Genomics Resource Center Gold collection but found sequence inconsistencies in it compared with the genome sequence. These inconsistencies were corrected in the cDNA before subcloning. The coding sequence was also cloned via Gateway into the pPWG vector to fuse GFP in frame to the last *cd* codon. P[acman] transgenes were integrated into the attP 51D site by Model System Genomics (Duke University). *P* element transgenes were integrated by standard procedures.

RNAi assays

The *GMR-wIR* transgene has been described in Lee and Carthew (2003). One copy of the *GMR-wIR* transgene partially silences *white* and generates a pale orange eye. The other transgenic RNAi lines (UAS-*argosIR*, UAS-*bwIR*, and UAS-*prIR*) were previously described in Dietzl et al. (2007), and *GMR-Gal4* was used to drive their expression specifically in the compound eye. UAS–*Dicer-2* transgenic lines were obtained from the Bloomington Stock Center and were coexpressed with RNAi transgenes to enhance their RNAi effects.

Quantification of eye pigments

The concentration of drosopterin and ommochrome pigments in adult heads was measured by the method previously described in Falcón-Pérez et al. (2007). Drosopterin was extracted from pools of four freshly dissected females heads (2–5 d old) by homogenization in 250 µl of 30% (volume/volume) ethanol (acidified to pH ~2 with HCl) followed by tumbling overnight at RT. The extracts were cleared twice by centrifugation for 1 min at 13,000 *g*, and their absorbance at 480 nm was measured against extracts prepared in parallel from w^{1118} fly heads, which were used as blank controls. To measure drosopterin in the presence of the *GMR-wIR* transgene, the number of fly heads was increased to 30, and the subsequent clarified solution was evaporated using speed vacuum and redissolved in 20 µl. Ommochrome was extracted from pools of eight freshly dissected heads except when in the presence of *GMR-wIR*, when the number of heads was increased to 30 and the extract was concentrated to 10 µl. Heads were homogenized in 150 µl of 2N HCl using a motorized pestle followed by an addition of 10 µl of 100-g/L sodium metabisulphite ($Na_2S_2O_5$) and 200 µl *n*-butanol and by tumbling for 1 h at RT. After centrifugation for 5 min at 4,000 *g*, the organic phase was washed using 150 µl of 0.66% (weight/volume) sodium metabisulphite, tumbled for 40 min at RT, and then centrifuged again. Subsequently, 145 µl of the washed organic phase was dried down in a speed vacuum. The pellet was dissolved in 10 µl ethanol, and absorbance was immediately measured at 490 nm against distilled water, which was used as a blank control. For both types of pigments, the resulting absorbance values were normalized to those obtained using FRT82B or Oregon-R.

Real-time quantitative PCR (qPCR)

Real-time qPCR was performed as described in Marques et al. (2010). Total RNA was extracted using TRIZOL reagent according to the manufacturer's protocol (Invitrogen). 100 ng–1 µg of total RNA was reverse transcribed using random primers and SuperScript Reverse Transcriptase (Invitrogen). The resulting cDNA was used as a template for qPCR reaction using Sybr green (Invitrogen) on an iCycler system (Bio-Rad Laboratories). The relative amount of the indicated RNAs normalized to an internal control was calculated using the ΔCt method (Rpl32). The primers used were as follows: *cd*, 5′-TGCTCAGCTGCATGGTGT-3′ and 5′-CGGCCAGACTGGTCTTGTA-3′; *w*, 5′-TCCTGACCAACATGACCTTTC-3′ and 5′-AAAAACTGGCAGCTCTGAGG-3′; *Rpl32*, 5′-GACGCTTCAAGGGACAGTATCTG-3′ and 5′-AAACGCGGTTCTGCATGAG-3′; *bw*, 5′-CGGCAGGATCGTCTACCA-3′ and 5′-TTCGTAGCCCAGGTCTGTAAA-3′; and *pr*, 5′-GATACGCGCTGCCTTGTTA-3′ and 5′-TTTTCTGTTGCAAGTGCCTATG-3′.

Cytoplasmic lysate preparation

Embryo lysates were prepared in lysis buffer (30 mM Hepes-KOH, pH 7.4, 100 mM potassium acetate, 2 mM magnesium acetate, 5 mM DTT, and Complete Mini Protease Inhibitor [Roche]) from 0–6-h-old embryos as described in Tuschl et al. (1999).

mRNA cleavage assay

Pp-luc mRNA was transcribed with T7 RNA polymerase to generate a 510-nt product. The transcript was then 7-methylguanosine capped using guanylyl transferase (Invitrogen) and γ-[^{32}P]GTP (MP Biomedicals) according to the manufacturer's instructions. The synthetic Pp-luc siRNA used in target mRNA cleavage was identical to that previously described (Pham et al., 2004). Duplex siRNA was prepared by annealing the single-stranded RNAs in annealing buffer for 1 h at 37°C after a 2-min incubation at 95°C. For target mRNA cleavage reactions, unlabeled siRNA was incubated with embryo lysate and labeled mRNA at 25°C as described in Pham et al. (2004). Products were resolved by electrophoresis on a 10% acrylamide-urea gel.

dsRNA processing assay

Pp-luc dsRNA was prepared by transcribing sense and antisense strands using T7 and SP6 RNA polymerase, respectively. Transcription reactions were performed in the presence of α-[^{32}P]UTP (MP Biomedicals) to give internally radiolabeled products 465-nt (sense) or 460-nt (antisense) long. The products were mixed 1:1 in annealing buffer (30 mM Hepes, pH 7.5, 100 mM potassium acetate, and 2 mM magnesium acetate), heated at 95°C for 2 min, and annealed overnight at 37°C to give duplex RNA. Reactions were performed mixing labeled dsRNA and embryo lysate at 25°C as described in Pham et al. (2004). Products were resolved by electrophoresis on a 15% acrylamide-urea gel. To quantitate processing, Phosphor Imager scans (Storm; GE Healthcare) were performed, and radioactive intensities of substrates and products were measured for each time point and subtracted for background.

Ago2 loading assay

Single-stranded Pp-luc siRNA oligonucleotides were 5′ end labeled with γ-[^{32}P]ATP (MP Biomedicals) and polynucleotide kinase before annealing to form an siRNA duplex. Reactions were performed by incubating embryo lysate with labeled siRNA in 5-µl RNAi reactions at 25°C for 40 min. The reactions were quenched with 1 µl heparin mix (60 mM potassium phosphate, 3 mM magnesium chloride, 3% PEG8000, 8% glycerol, and 4 mg/ml heparin), yielding a final heparin concentration of 0.67 mg/ml. They were then loaded onto a prechilled 4% (40:1 acrylamide/bisacrylamide) native gel and run at 4°C in 1× Tris/Borate/EDTA at 10 W. The gel was dried and exposed to a Phosphor Imager overnight.

S2 cell experiments

Using Gateway, *cd* cDNA was used to recombine the *cd* ORF into the pAWR vector, generating a carboxy-terminally tagged RFP construct for expression in S2 cells. The construct was under Actin5c promoter control. A stable cell line expressing constitutive Lamp-1::GFP was a gift from V. Gelfand (Northwestern University, Chicago, IL). Cells were transfected using Cellfectin (Invitrogen) and harvested 24 h after transfection. Before fixation, cells were transferred onto poly-L-lysine coverslips. Cells were fixed with 2% PFA in PBS at RT. After washes, coverslips were mounted in Vectashield mounting medium (Vector Laboratories).

In situ fluorescence

Pupae carrying *GMR-Gal4; UAS-Cd::GFP* transgenes were dissected at 52 h after pupariation at 22°C. Eyes were fixed in 4% PFA/PBS at RT. After washes in PBS, they were mounted in Vectashield.

Microscopy

Adult eyes were examined on intact frozen flies by scanning electron or light microscopy. A scanning electron microscope (S-3400N-II; Hitachi) was used on mounted but noncoated specimens under variable chamber pressure. Images were acquired with the Hitachi software and exported into TIF format for Photoshop (Adobe). For light microscopy, a binocular microscope (SV-6; Carl Zeiss) was used on specimens, and images were acquired with Axiocam (Carl Zeiss) and AxioVision (Carl Zeiss) software. S2 cells and pupal eye tissue specimens were viewed under a confocal microscope (LSM510; Carl Zeiss) using a 63× objective (NA 1.4 oil immersion) at RT. Laser-scanning microscope acquisition software (Carl Zeiss) was used. Z sections of 0.5-µm thickness were captured as 1,024 × 1,024–pixel images with line averaging. Images were transferred into TIF format and rendered in Photoshop CS3.

Online supplemental material

Fig. S1 shows how pigmentation genes regulate *white*(RNAi). Fig. S2 highlights the conserved domains in Cd. Fig. S3 shows that Cd repression of *white*(RNAi) requires Dicer-2. Fig. S4 does not find a genetic interaction between *cd* and *argos*. Fig. S5 shows the mRNA expression of *cd* in different *Drosophila* tissues. Online supplemental material is available at http://www.jcb.org/cgi/content/full/jcb.201102021/DC1.

We thank Desmond Watt for help with Cd localization in eye tissue. We thank V. Gelfand for the stable cell line expressing constitutive Lamp-1::GFP. Stocks were obtained from the Bloomington Stock Center, RNAi lines were obtained from the Vienna Drosophila RNAi Center, and cDNA was obtained from the Drosophila Genome Resource Center.

D.A. Harris was supported by a Damon Runyon postdoctoral fellowship and a traineeship from the Oncogenesis and Developmental Biology T32 Training grant. This work was also supported by the National Institutes of Health (GM068943).

Submitted: 4 February 2011
Accepted: 7 June 2011

References

Bernstein, E., A.A. Caudy, S.M. Hammond, and G.J. Hannon. 2001. Role for a bidentate ribonuclease in the initiation step of RNA interference. *Nature*. 409:363–366. doi:10.1038/35053110

Bonifacino, J.S., and B.S. Glick. 2004. The mechanisms of vesicle budding and fusion. *Cell*. 116:153–166. doi:10.1016/S0092-8674(03)01079-1

Carthew, R.W., and E.J. Sontheimer. 2009. Origins and mechanisms of miRNAs and siRNAs. *Cell*. 136:642–655. doi:10.1016/j.cell.2009.01.035

Cheli, V.T., R.W. Daniels, R. Godoy, D.J. Hoyle, V. Kandachar, M. Starcevic, J.A. Martinez-Agosto, S. Poole, A. DiAntonio, V.K. Lloyd, et al. 2010.

Genetic modifiers of abnormal organelle biogenesis in a *Drosophila* model of BLOC-1 deficiency. *Hum. Mol. Genet.* 19:861–878. doi:10.1093/hmg/ddp555

Chiang, P.W., N. Oiso, R. Gautam, T. Suzuki, R.T. Swank, and R.A. Spritz. 2003. The Hermansky-Pudlak syndrome 1 (HPS1) and HPS4 proteins are components of two complexes, BLOC-3 and BLOC-4, involved in the biogenesis of lysosome-related organelles. *J. Biol. Chem.* 278:20332–20337. doi:10.1074/jbc.M300090200

Cikaluk, D.E., N. Tahbaz, L.C. Hendricks, G.E. DiMattia, D. Hansen, D. Pilgrim, and T.C. Hobman. 1999. GERp95, a membrane-associated protein that belongs to a family of proteins involved in stem cell differentiation. *Mol. Biol. Cell*. 10:3357–3372.

Dietzl, G., D. Chen, F. Schnorrer, K.C. Su, Y. Barinova, M. Fellner, B. Gasser, K. Kinsey, S. Oppel, S. Scheiblauer, et al. 2007. A genome-wide transgenic RNAi library for conditional gene inactivation in *Drosophila*. *Nature*. 448:151–156. doi:10.1038/nature05954

Di Pietro, S.M., and E.C. Dell'Angelica. 2005. The cell biology of Hermansky-Pudlak syndrome: recent advances. *Traffic*. 6:525–533. doi:10.1111/j.1600-0854.2005.00299.x

Elbashir, S.M., W. Lendeckel, and T. Tuschl. 2001. RNA interference is mediated by 21- and 22-nucleotide RNAs. *Genes Dev.* 15:188–200. doi:10.1101/gad.862301

Falcón-Pérez, J.M., R. Nazarian, C. Sabatti, and E.C. Dell'Angelica. 2005. Distribution and dynamics of Lamp1-containing endocytic organelles in fibroblasts deficient in BLOC-3. *J. Cell Sci.* 118:5243–5255. doi:10.1242/jcs.02633

Falcón-Pérez, J.M., R. Romero-Calderón, E.S. Brooks, D.E. Krantz, and E.C. Dell'Angelica. 2007. The *Drosophila* pigmentation gene pink (p) encodes a homologue of human Hermansky-Pudlak syndrome 5 (HPS5). *Traffic*. 8:154–168. doi:10.1111/j.1600-0854.2006.00514.x

Feng, L., E.K. Novak, L.M. Hartnell, J.S. Bonifacino, L.M. Collinson, and R.T. Swank. 2002. The Hermansky-Pudlak syndrome 1 (HPS1) and HPS2 genes independently contribute to the production and function of platelet dense granules, melanosomes, and lysosomes. *Blood*. 99:1651–1658. doi:10.1182/blood.V99.11.4006

Gibbings, D.J., C. Ciaudo, M. Erhardt, and O. Voinnet. 2009. Multivesicular bodies associate with components of miRNA effector complexes and modulate miRNA activity. *Nat. Cell Biol.* 11:1143–1149. doi:10.1038/ncb1929

Haley, B., G. Tang, and P.D. Zamore. 2003. In vitro analysis of RNA interference in *Drosophila melanogaster*. *Methods*. 30:330–336. doi:10.1016/S1046-2023(03)00052-5

Hartmann, E., T.A. Rapoport, and H.F. Lodish. 1989. Predicting the orientation of eukaryotic membrane-spanning proteins. *Proc. Natl. Acad. Sci. USA*. 86:5786–5790. doi:10.1073/pnas.86.15.5786

Hirosaki, K., T. Yamashita, I. Wada, H.Y. Jin, and K. Jimbow. 2002. Tyrosinase and tyrosinase-related protein 1 require Rab7 for their intracellular transport. *J. Invest. Dermatol.* 119:475–480. doi:10.1046/j.1523-1747.2002.01832.x

Howells, A.J., K.M. Summers, and R.L. Ryall. 1977. Developmental patterns of 3-hydroxykynurenine accumulation in white and various other eye color mutants of *Drosophila melanogaster*. *Biochem. Genet.* 15:1049–1059. doi:10.1007/BF00484496

Huizing, M., A. Helip-Wooley, W. Westbroek, M. Gunay-Aygun, and W.A. Gahl. 2008. Disorders of lysosome-related organelle biogenesis: clinical and molecular genetics. *Annu. Rev. Genomics Hum. Genet.* 9:359–386. doi:10.1146/annurev.genom.9.081307.164303

Jordens, I., W. Westbroek, M. Marsman, N. Rocha, M. Mommaas, M. Huizing, J. Lambert, J.M. Naeyaert, and J. Neefjes. 2006. Rab7 and Rab27a control two motor protein activities involved in melanosomal transport. *Pigment Cell Res.* 19:412–423. doi:10.1111/j.1600-0749.2006.00329.x

Kim, K., Y.S. Lee, and R.W. Carthew. 2007. Conversion of pre-RISC to holo-RISC by Ago2 during assembly of RNAi complexes. *RNA*. 13:22–29. doi:10.1261/rna.283207

Krämer, H. 2002. Sorting out signals in fly endosomes. *Traffic*. 3:87–91. doi:10.1034/j.1600-0854.2002.030201.x

Lee, Y.-S., and R.W. Carthew. 2003. Making a better RNAi vector for *Drosophila*: use of intron spacers. *Methods*. 30:322–329. doi:10.1016/S1046-2023(03)00051-3

Lee, Y.S., K. Nakahara, J.W. Pham, K. Kim, Z. He, E.J. Sontheimer, and R.W. Carthew. 2004. Distinct roles for *Drosophila* Dicer-1 and Dicer-2 in the siRNA/miRNA silencing pathways. *Cell*. 117:69–81. doi:10.1016/S0092-8674(04)00261-2

Lee, Y.S., S. Pressman, A.P. Andress, K. Kim, J.L. White, J.J. Cassidy, X. Li, K. Lubell, H. Lim, I.S. Cho, et al. 2009. Silencing by small RNAs is linked to endosomal trafficking. *Nat. Cell Biol.* 11:1150–1156. doi:10.1038/ncb1930

Lloyd, V., M. Ramaswami, and H. Krämer. 1998. Not just pretty eyes: *Drosophila* eye-colour mutations and lysosomal delivery. *Trends Cell Biol.* 8:257–259. doi:10.1016/S0962-8924(98)01270-7

Lugli, G., J. Larson, M.E. Martone, Y. Jones, and N.R. Smalheiser. 2005. Dicer and eIF2c are enriched at postsynaptic densities in adult mouse brain and are modified by neuronal activity in a calpain-dependent manner. *J. Neurochem.* 94:896–905. doi:10.1111/j.1471-4159.2005.03224.x

Ma, J., H. Plesken, J.E. Treisman, I. Edelman-Novemsky, and M. Ren. 2004. Lightoid and Claret: a rab GTPase and its putative guanine nucleotide exchange factor in biogenesis of *Drosophila* eye pigment granules. *Proc. Natl. Acad. Sci. USA*. 101:11652–11657. doi:10.1073/pnas.0401926101

Mackenzie, S.M., A.J. Howells, G.B. Cox, and G.D. Ewart. 2000. Sub-cellular localisation of the white/scarlet ABC transporter to pigment granule membranes within the compound eye of *Drosophila melanogaster*. *Genetica*. 108:239–252. doi:10.1023/A:1004115718597

Marques, J.T., K. Kim, P.H. Wu, T.M. Alleyne, N. Jafari, and R.W. Carthew. 2010. Loqs and R2D2 act sequentially in the siRNA pathway in *Drosophila*. *Nat. Struct. Mol. Biol.* 17:24–30. doi:10.1038/nsmb.1735

Martina, J.A., K. Moriyama, and J.S. Bonifacino. 2003. BLOC-3, a protein complex containing the Hermansky-Pudlak syndrome gene products HPS1 and HPS4. *J. Biol. Chem.* 278:29376–29384. doi:10.1074/jbc.M301294200

Nazarian, R., J.M. Falcón-Pérez, and E.C. Dell'Angelica. 2003. Biogenesis of lysosome-related organelles complex 3 (BLOC-3): a complex containing the Hermansky-Pudlak syndrome (HPS) proteins HPS1 and HPS4. *Proc. Natl. Acad. Sci. USA*. 100:8770–8775. doi:10.1073/pnas.1532040100

Nguyen, T., E.K. Novak, M. Kermani, J. Fluhr, L.L. Peters, R.T. Swank, and M.L. Wei. 2002. Melanosome morphologies in murine models of hermansky-pudlak syndrome reflect blocks in organelle development. *J. Invest. Dermatol.* 119:1156–1164. doi:10.1046/j.1523-1747.2002.19535.x

Nolte, D.J. 1961. The pigment granules in the compound eyes of *Drosophila*. *Heredity*. 16:25–38. doi:10.1038/hdy.1961.2

Pham, J.W., J.L. Pellino, Y.S. Lee, R.W. Carthew, and E.J. Sontheimer. 2004. A Dicer-2-dependent 80s complex cleaves targeted mRNAs during RNAi in *Drosophila*. *Cell*. 117:83–94. doi:10.1016/S0092-8674(04)00258-2

Raposo, G., and M.S. Marks. 2007. Melanosomes—dark organelles enlighten endosomal membrane transport. *Nat. Rev. Mol. Cell Biol.* 8:786–797. doi:10.1038/nrm2258

Raposo, G., M.S. Marks, and D.F. Cutler. 2007. Lysosome-related organelles: driving post-Golgi compartments into specialisation. *Curr. Opin. Cell Biol.* 19:394–401. doi:10.1016/j.ceb.2007.05.001

Schwarz, D.S., G. Hutvágner, T. Du, Z. Xu, N. Aronin, and P.D. Zamore. 2003. Asymmetry in the assembly of the RNAi enzyme complex. *Cell*. 115:199–208. doi:10.1016/S0092-8674(03)00759-1

Schwarz, D.S., Y. Tomari, and P.D. Zamore. 2004. The RNA-induced silencing complex is a Mg2+-dependent endonuclease. *Curr. Biol.* 14:787–791. doi:10.1016/j.cub.2004.03.008

Sevrioukov, E.A., J.P. He, N. Moghrabi, A. Sunio, and H. Krämer. 1999. A role for the deep orange and carnation eye color genes in lysosomal delivery in *Drosophila*. *Mol. Cell*. 4:479–486. doi:10.1016/S1097-2765(00)80199-9

Shoup, J.R. 1966. The development of pigment granules in the eyes of wild type and mutant *Drosophila melanogaster*. *J. Cell Biol.* 29:223–249. doi:10.1083/jcb.29.2.223

Siddiqui, S.S., and P. Babu. 1980. Kynurenine hydroxylase mutants of the nematode *Caenorhabditis elegans*. *Mol. Gen. Genet.* 179:21–24. doi:10.1007/BF00268441

Suzuki, T., W. Li, Q. Zhang, A. Karim, E.K. Novak, E.V. Sviderskaya, S.P. Hill, D.C. Bennett, A.V. Levin, H.K. Nieuwenhuis, et al. 2002. Hermansky-Pudlak syndrome is caused by mutations in HPS4, the human homolog of the mouse light-ear gene. *Nat. Genet.* 30:321–324.

Syrzycka, M., L.A. McEachern, J. Kinneard, K. Prabhu, K. Fitzpatrick, S. Schulze, J.M. Rawls, V.K. Lloyd, D.A. Sinclair, and B.M. Honda. 2007. The pink gene encodes the *Drosophila* orthologue of the human Hermansky-Pudlak syndrome 5 (HPS5) gene. *Genome*. 50:548–556. doi:10.1139/G07-032

Tomari, Y., C. Matranga, B. Haley, N. Martinez, and P.D. Zamore. 2004. A protein sensor for siRNA asymmetry. *Science*. 306:1377–1380. doi:10.1126/science.1102755

Tuschl, T., P.D. Zamore, R. Lehmann, D.P. Bartel, and P.A. Sharp. 1999. Targeted mRNA degradation by double-stranded RNA in vitro. *Genes Dev.* 13:3191–3197. doi:10.1101/gad.13.24.3191

Venken, K.J., Y. He, R.A. Hoskins, and H.J. Bellen. 2006. P[acman]: a BAC transgenic platform for targeted insertion of large DNA fragments in *D. melanogaster*. *Science*. 314:1747–1751. doi:10.1126/science.1134426

Wei, M.L. 2006. Hermansky-Pudlak syndrome: a disease of protein trafficking and organelle function. *Pigment Cell Res.* 19:19–42. doi:10.1111/j.1600-0749.2005.00289.x